Available online at www.sciencedirect.com

ScienceDirect

journal homepage: http://www.elsevier.com/locate/jab

Original Research Article

Study on novel, superparamagnetic and biocompatible PEG/$KFeO_2$ nanocomposite

Lavanya Khanna *, *Narendra Kumar Verma*

Nano Research Lab, School of Physics and Materials Science, Thapar University, Patiala 147004, India

ARTICLE INFO

Article history:
Received 6 January 2014
Received in revised form
10 May 2014
Accepted 20 May 2014
Available online 2 June 2014

Keywords:
PEG
Potassium ferrite nanoparticles
Nanocomposite
Superparamagnetic
Biocompatible

ABSTRACT

The present study reports the synthesis of polyethylene glycol (PEG) coated potassium ferrite nanoparticles. X-ray diffraction pattern revealed the formation of orthorhombic structure of $KFeO_2$ nanoparticles, along with additional characteristic peaks of PEG at 2θ ~19° and 23°. The characteristic IR bands of PEG confirmed its coating thereby making the nanocomposite feasible for bio-conjugation. The coating of PEG on $KFeO_2$ nanoparticles, spherical formation, and reduced agglomeration of the nanocomposite were revealed by high resolution transmission electron microscope, transmission electron microscope and scanning electron microscope studies, respectively. In vibrating sample magnetometer analysis, the synthesized nanocomposite exhibited superparamagnetic behavior with magnetic saturation value of 5.78 emu/g and high biocompatibility below 250 μg/ml.

Introduction

Magnetic nanoparticles (MNPs) such as Fe_3O_4 (Zhang et al., 2008; Tomitaka et al., 2009; Yallapu et al., 2011), $NiFe_2O_4$ (Yin et al., 2005; Rana et al., 2007; Tomitaka et al., 2009), $MnFe_2O_4$ (Leung and Wang, 2010; Yang et al., 2010), $CoFe_2O_4$ (Baldi et al., 2007; Rana et al., 2010; Mohapatra et al., 2011), $ZnFe_2O_4$ (Tomitaka et al., 2009) find wide applications in biomedicine. Although ferrites of Ni, Mn, Co, Zn possess good magnetic properties, their inherent toxicity weakens their reliability. This raises apprehensions on their efficacy and biocompatibility for biomedical applications. Ferrites of potassium are expected to be more biocompatible since potassium is inherently non-toxic. Going through the literature, reports on potassium ferrite compounds in bulk form are available wherein these have been used for dyeing, waste-water purification, and disinfection (Jiang et al., 2006; Ciabatti et al., 2010; Lim and Kim, 2010; Ling et al., 2010).

For biomedicinal applications, there are certain prerequisites such as nanosize, superparamagnetism, and biocompatibility. Particles with diameters greater than 200 nm are usually mechanically filtered and sequestered by the spleen. Also, the chances of larger particles clogging the small capillaries become significant (Larumbe et al., 2012; Mukhopadhyay et al., 2012). Smaller particles with size less than 5 nm are quickly removed through extravasations and renal clearance. Therefore, particles ranging from 5 to 100 nm are optimal for intravenous injection owing to their most prolonged blood circulation time. Also, the particles within this size range are small enough both to escape Reticuloendothelial system (RES) of the body and to penetrate the very small

* *Corresponding author*. Tel.: +91 0175 2393343; fax: +91 0175 2364498/2393002.
E-mail addresses: lavanshya@yahoo.co.in, lavanya.khanna@thapar.edu, lavanshya@gmail.com (L. Khanna).
1214-021X/$ – see front matter
http://dx.doi.org/10.1016/j.jab.2014.05.003

capillaries. This rules out the possibility of clogging the capillaries and offers the most effective distribution in the body. In addition, they have higher effective surface area (easier attachment of ligands), lower sedimentation rates (high stability), and improved tissular diffusion; this shows the preferred size lies in the range of 5–100 nm (Larumbe et al., 2012). The other requirement is that the particles must exhibit superparamagnetic behavior. Another requirement is superparamagnetism; superparamagnetic nanoparticles become magnetic in the presence of an external magnetic field but return to a nonmagnetic state on its removal. Unlike ferromagnetic particles, which retain magnetism even after removal of magnetic field. This avoids their 'active' behavior in the absence of field, and such behavior is ideal for biomedical applications. In general, a localized magnetic field gradient is used for attracting and retaining the nanoparticles to a selected site until the completion of the therapy leading to their removal (Koo et al., 2005; Schulz et al., 2009). The advantage of using superparamagnetic nanoparticles for this application underlies the fact that the applied magnetic field triggers response for its planned action, which stops as soon as the magnetic field is removed; consequently, enabling control on their planned action and time of exposure.

The fate of nanoparticles is dependent on other factors as well. Like, pertaining to high surface energy and magnetic interactions, they have the tendency to agglomerate. On agglomeration, they adsorb plasma proteins, and are quickly cleared by the macrophages in the reticuloendothelial system (a part of the immune system of the human body) before reaching the target cells (Gupta and Gupta, 2005). Human body works against the nanoparticles by clearing them prior to their planned action, thus, reducing their circulation time in the blood stream. Also, the surface inertness of nanoparticles limits their bio-conjugation (Sun et al., 2005; Čampelj et al., 2009). All these factors make coating indispensable for their effective working. For coating, polymers are widely used as they reduce agglomeration, help in evading the reticuloendothelial system, and facilitate the selective binding of the biological entities. In addition, the polymer prevents the corrosion of the ferrite surface thereby making it more biocompatible.

Considering all the above facts, the formation of magnetic polymer nanocomposite (magnetic core with a polymer coating on its surface (McBain et al., 2008)) is essential for their application in biomedicine. The widely used polymer is Polyethylene Glycol (PEG) – a polymer of ethylene oxide and water with the general formula H (OCH_2CH_2) nOH, where n is the average number of repeating (OCH_2CH_2) groups ranging between 4 and 180. It is typically a non-toxic, non-immunogenic, non-antigenic, protein resistant polymer, and, is widely used in pharmaceutical field (Veiseh et al., 2010; Mukhopadhyay et al., 2012). It is water soluble, inert in biological systems, and does not influence cell viability (Feng et al., 2008; Ahmed et al., 2010). PEGylated nanoparticles improve stealth properties unparalleled by any other surface coating (Rastogi et al., 2011). PEG displays little toxicity and immunogenicity and the complete removal is either through kidneys (for PEG $<$ 30 kDa) or in feces (for PEG $>$ 20 kDa) (Arruebo et al., 2007); it serves as a protective layer that prevents agglomeration of the particles, thereby providing protection against corrosion, evading reticuloendothelial system (RES), helping in binding various biological ligands to the nanoparticle surface, and minimizing the direct exposure of the ferrite surface to the biological environment. This consequently enhances biocompatibility (Ahmed et al., 2010; Veiseh et al., 2010). The ordered and uniform chain structure of PEG allows its easy absorption at the surface of the nanoparticles (Karaoglu et al., 2011). It is imperative to optimize the coating as the immunostealthing provided by PEG is concomitant with loss of bio-molecular targeting capabilities and magnetic degradation (Feng et al., 2008).

PEG coated nanocomposites as Mn_3O_4 (Durmus et al., 2011; Karaoglu et al., 2011), Au (Lipka et al., 2010; Zhang et al., 2011), Ag (Tejamaya et al., 2012), silica (Echevarria et al., 2010; Singh et al., 2011), have been reported. In addition, ferrites as $NiFe_2O_4$ (Ma et al., 2010), $MnFe_2O_4$ (Phadatare et al., 2012), Fe_3O_4 (Feng et al., 2008; Zhang et al., 2008; Lee et al., 2011; Mukhopadhyay et al., 2012), have also been coated with PEG. Zhang et al. (2011) studied size-dependent (5, 10, 30 and 60 nm) *in vivo* toxicity of PEG-coated gold nanoparticles in mice. The toxicity of 10 nm and 60 nm particles was found to be higher than that of 5 nm and 30 nm particles – the former ones registered slight damage to the liver. Rastogi et al. (2011) studied folate conjugated PEGylated thermosensitive magnetic nanocomposites. MTT assay cell viability studied at 20 and 40 μg/ml revealed their dose-dependent cytotoxicity, and, at higher concentration, significant cell death was observed (∼80%). Sun et al. (2010) studied hepatotoxicity assay of PEG-mediated superparamagnetic nanoparticles (ION/PEG), and observed that it did not elicit any apparent toxic effects. Lim et al. (2008) synthesized various types of water soluble PEGylated magnetic complexes (PMCs – (mPEG-lauric acid (PLMs)), (mPEG-stearic acid (PSMs)), and (mPEG-oleic acid (POMs))), and studied their cell viabilities for 48 h at various concentrations (0.06–7.82 μg/ml) on Hela cells. The results indicated that PMCs efficiently internalized into the Hela cells.

Studies on PEG coated potassium ferrite nanoparticles so far have not been investigated. The motivation of the present work was to synthesize and study PEG coated potassium ferrite nanoparticles for biomedical applications. Along with the synthesis, the structural, morphological, thermal, magnetic, FTIR, and cytotoxicity properties of PEG coated potassium ferrite nanoparticles have been studied and discussed.

Materials and methods

Materials

All the chemicals used for synthesis were of analytical grade. Potassium nitrate KNO_3, Ferric nitrate ($Fe(NO_3)_3{\cdot}9H_2O$), and citric acid ($C_6H_8O_7{\cdot}H_2O$), were purchased from Loba Chemie, India, ethylene glycol was purchased from Sdfine chemicals, India and were used without any further purifications.

Synthesis of PEG coated potassium ferrite nanoparticles

Sol–gel method was employed for the synthesis of bare potassium ferrite nanoparticles. 1 M solution of potassium

nitrate, 2 M solution of ferric nitrate and 2 M citric acid solution were mixed along with 7 ml of ethylene glycol. The solution was constantly magnetically stirred at 80–90 °C. In the process of heating and stirring, formations of sol, gel, dried gel and finally powder were obtained. The obtained powder was thoroughly washed with ethanol by centrifugation at 2000 rpm and dried overnight in vacuum oven at 60 °C. The dried powder was grinded in pestle and mortar and further calcined to obtain the ferrite nanoparticles. To synthesize PEG coated potassium ferrite nanoparticles, nanoparticles were mixed with the PEG (Molecular Weight 1500) solution with the concentration of 0.01 g/ml, followed by addition of a certain amount of ammonia solution until the pH of the solution reached 11. After continuous stirring, a homogeneous mixture was obtained. The mixture was poured into a Teflon lined stainless-steel autoclave (50 ml), kept at 140 °C for 12 h, and then cooled to room temperature naturally (Gozuak et al., 2009). The obtained product was washed several times with ethanol; finally, it was dried overnight in a vacuum oven at 60 °C. The dried powder was grinded in pestle and mortar to obtain uniform fine powder. Fig. 1 depicts the schematic of PEG coating on ferrite nanoparticles (Zhang et al., 2008).

Statistical analysis

The statistical analysis of the experimental data of the synthesized nanocomposite was done by Student's paired *t*-test. Results are expressed as mean ± standard error. Experimental data were evaluated at the significance level $2\alpha = 0.05$.

Characterizations

Structure, morphology and particle size

The structure and morphology of synthesized nanocomposite were studied by X-ray diffraction (XRD: X'PERT PRO Panalytical, MRD ML) and Scanning Electron Microscope (SEM: JSM, 6510 LV, JEOL, USA) where the dried sample was first coated with gold using JEOL, JFC sputter coater. The particle size was determined by transmission electron microscope (TEM: Hitachi (H-7500)). The HRTEM image was obtained by High-resolution transmission electron microscope (TEM – JEOL 2100F).

Fourier transform infrared spectroscopy

The FTIR spectrum of the powdered nanoparticles pressed into 13 mm thick KBr pellets, in the frequency range 4000 cm^{-1} to 400 cm^{-1}, was recorded on Perkin Elmer-Model RZX.

Thermal analysis

The thermal analysis was done with differential thermal analyzer (DTA: Pyris 1 TGA, Perkin Elmer).

Magnetic analysis

The magnetic properties and saturation magnetization was determined using vibrating sample magnetometer (VSM: Princeton Applied Research Model 151/155).

In vitro cytotoxicity

The viability of T cell lines (Jurkat cells) incubated with PEG coated potassium ferrite nanoparticles at different concentrations, was investigated by MTT (3-(4,5-dimethylthiazol-2-yl)-2,5-diphenyltetrazolium bromide, a tetrazole) colorimetric assay. Cells were cultured on tissue culture polystyrene falcon flasks in RPMI-1640 supplemented by 10% FCS (Fetal Calf Serum) at 37 °C in 5% CO_2. This solution was then centrifuged at 1200 rpm at 4 °C for 5 min to separate dead cells. The cells were trypsinized and counted on haemocytometer. After trypsinization, the cells in media were placed in 96-well tissue culture flat bottom plate at a density of 1.5×10^4 cells per well. Required concentration (5, 25, 50, 100, 250, 500 μg/ml) of nanoparticles ($n = 4$) was added to the wells. It was then incubated for 48 h in CO_2 incubator at 37 °C in 5% CO_2. Controls were carried out consisting of growing cells without any treatment. After 48 h, the cell suspension was removed from each well. Thereafter, the cell suspension, after adding to it 20 μl of MTT solution, was incubated for 4–5 h. Viable cells have the ability to reduce yellow MTT to insoluble purple formazan; this reduction takes place only when mitochondrial reductase enzymes are active, and, therefore, conversion can be directly related to the number of viable (living) cells. Reaction was stopped by addition of stop lysis solution (20% SDS in 50% dimethyl formamide + 50% distilled water). Plates were further incubated for 1 h and absorbance was recorded at

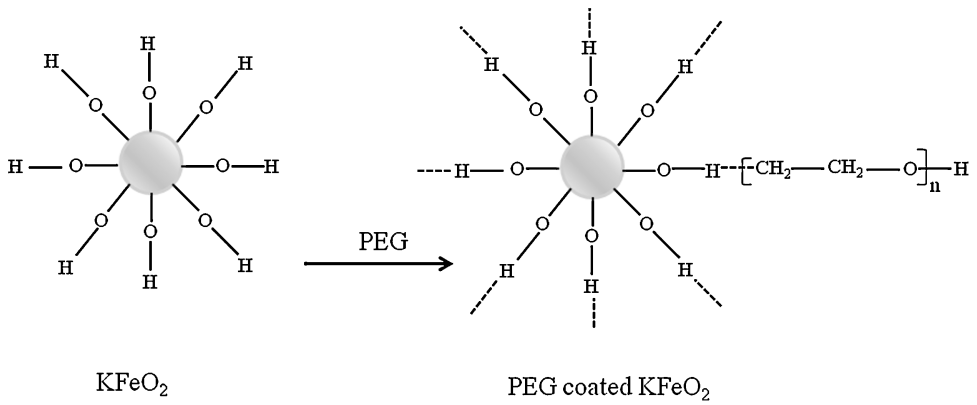

Fig. 1 – Schematic of PEG coating on potassium ferrite nanoparticles.

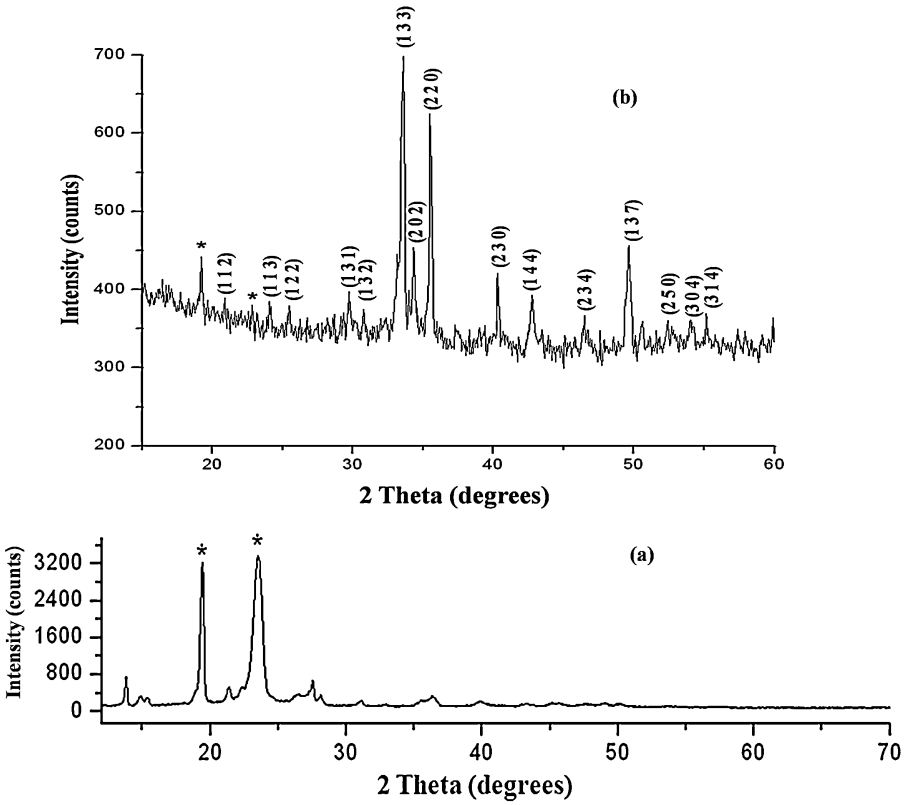

Fig. 2 – XRD pattern of (a) PEG and (b) PEG coated potassium ferrite nanoparticles.

570 nm on ELISA Plate Reader. Mean and standard deviation was obtained from 5 replicates.

Cell viability was calculated by the following formula, Eq. (1):

$$\text{Cell viability}\,(\%) = \left(\frac{I_{\text{sample}}}{I_{\text{control}}}\right) * 100 \quad (1)$$

I_{sample} is the absorbance of nanoparticles treated wells and I_{control} is the absorbance of control wells without nanoparticles treatment (Rastogi et al., 2011).

Results and discussion

Structural analysis

The XRD pattern of PEG in Fig. 2(a) reveals two distinct peaks at 19° and 23° (marked as *), characteristic of its crystalline nature. Fig. 2(b) shows the XRD pattern of PEG coated potassium ferrite nanoparticles – two peaks at ~19° and 23° – characteristic of PEG, have been observed (marked as *), confirming the presence of PEG (Khanna and Verma, 2013a,b). All the other peaks are attributed to the formation of orthorhombic structure (File No. 83-2152, space group: Pbca) of $KFeO_2$. The sharpening of the peaks is due to the increase in the size after PEG coating; this is also confirmed by the TEM analysis. The lattice parameters were calculated at measurement wavelength 1.54060 Å using the diffraction peaks (1 3 3), (2 2 0), (1 3 7). Table 1 gives the theoretical and calculated values of the unit cell parameters.

Table 1 – Theoretical and calculated values of the unit cell parameters.

PEG coated $KFeO_2$				
		Theoretical	Calculated	Difference
Unit cell parameters	a	5.577	5.706	0.129
	b	11.220	10.940	0.279
	c	15.890	15.910	0.024

FTIR analysis

FTIR spectroscopy was performed to understand the modification of the nanoparticles by the PEG molecules.

Table 2 – Description of FTIR spectrum of PEG coated potassium ferrite nanoparticles.

IR band (cm^{-1})	Description
3426	ν(OH) stretching
1631	ν(OH) bending
1384	$w(CH_2)$ wagging
1271	ν(OH) bending and $\tau(CH_2)$ twisting
1091	ν(C–O–C) ether stretching
693	ν (Fe–OH) stretching
636, 586, 482	ν(Fe–O) stretching

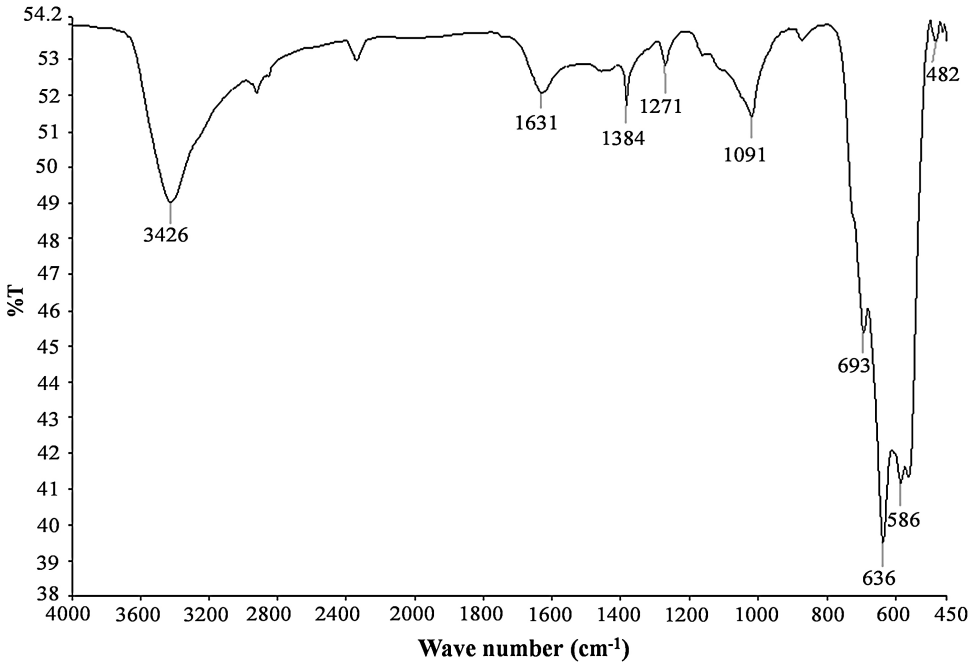

Fig. 3 – FTIR spectrum of PEG coated potassium ferrite nanoparticles.

In the FTIR spectrum of PEG coated potassium ferrite nanoparticles, Fig. 3, the broad stretches at 3426 cm^{-1} and 1631 cm^{-1} are due to O–H stretching and O–H bending vibrations, respectively (Silverstein et al., 2005; Zampori et al., 2012). The band corresponding to molecular water in PEG is usually centered at 1644 cm^{-1}. But in the synthesized nanocomposite, it is formed at a slighter lower wave number. This is attributed to partial loss of water molecules due to surface coating of PEG (Zampori et al., 2012). The vibrations of C–H (wagging) at 1384 cm^{-1}, the bending vibrations of O–H and C–H (twisting) stretch at 1271 cm^{-1}, and a sharp C–O–C ether stretch at 1091 cm^{-1} clearly confirm the presence of PEG on potassium ferrite nanoparticles (Silverstein et al., 2005; Rastogi et al., 2011; Mukhopadhyay et al., 2012; Zampori et al., 2012). The bands due to C–H vibrational modes and water are strongly reudced in intensity due to dehydroxilation and oxidation of the organic moieties (Zampori et al., 2012). In the lower region, the band at 693 cm^{-1} is attributed to stretching vibrations of Fe–OH bond. The bands at 636, 586, 482 cm^{-1} correspond to Fe–O stretching bond (Rana et al., 2010). Table 2 shows the description of the bands for PEG coated potassium ferrite nanoparticles.

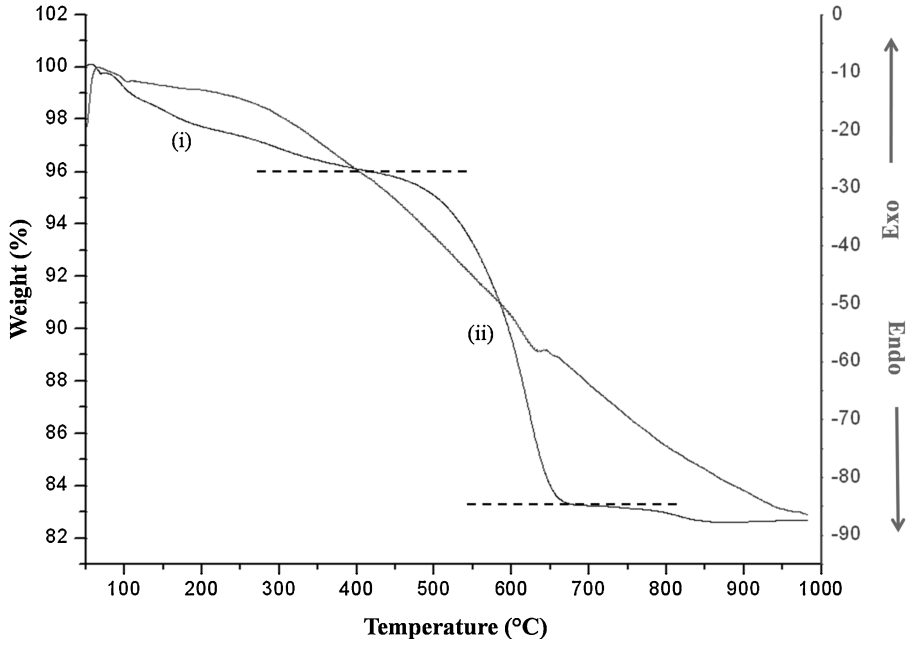

Fig. 4 – TGA and DTA curves of PEG coated potassium ferrite nanoparticles. (For colour resolution see the online edition.)

Thermal analysis

The decomposition of PEG coated potassium ferrite nanoparticles, Fig. 4, comprises of two distinct weight loss regions (i) ~50–400 °C, (ii) ~400–660 °C, denoted by black dashed lines. The first loss (~4%) corresponds to the release of the adsorbed water on the surface of the nanocomposite. The second weight loss (~14%) corresponds to the decomposition of PEG molecules, possibly due to the loss of organic hydrogen (Zampori et al., 2012). No significant peak has been observed in the DTA curve. Temperature, at which the weight of the PEG polymer significantly decreases, is shifted to higher temperature, indicating the enhanced thermal stability of PEG due to the formation of covalent bonds with potassium ferrite nanoparticles.

Morphological analysis

The spherical formation and reduced agglomeration of the synthesized nanocomposite is well-evident from Fig. 5(a–c). The reduced agglomeration is due to the surface coating of PEG, which reduces the surface interaction of the nanoparticles,

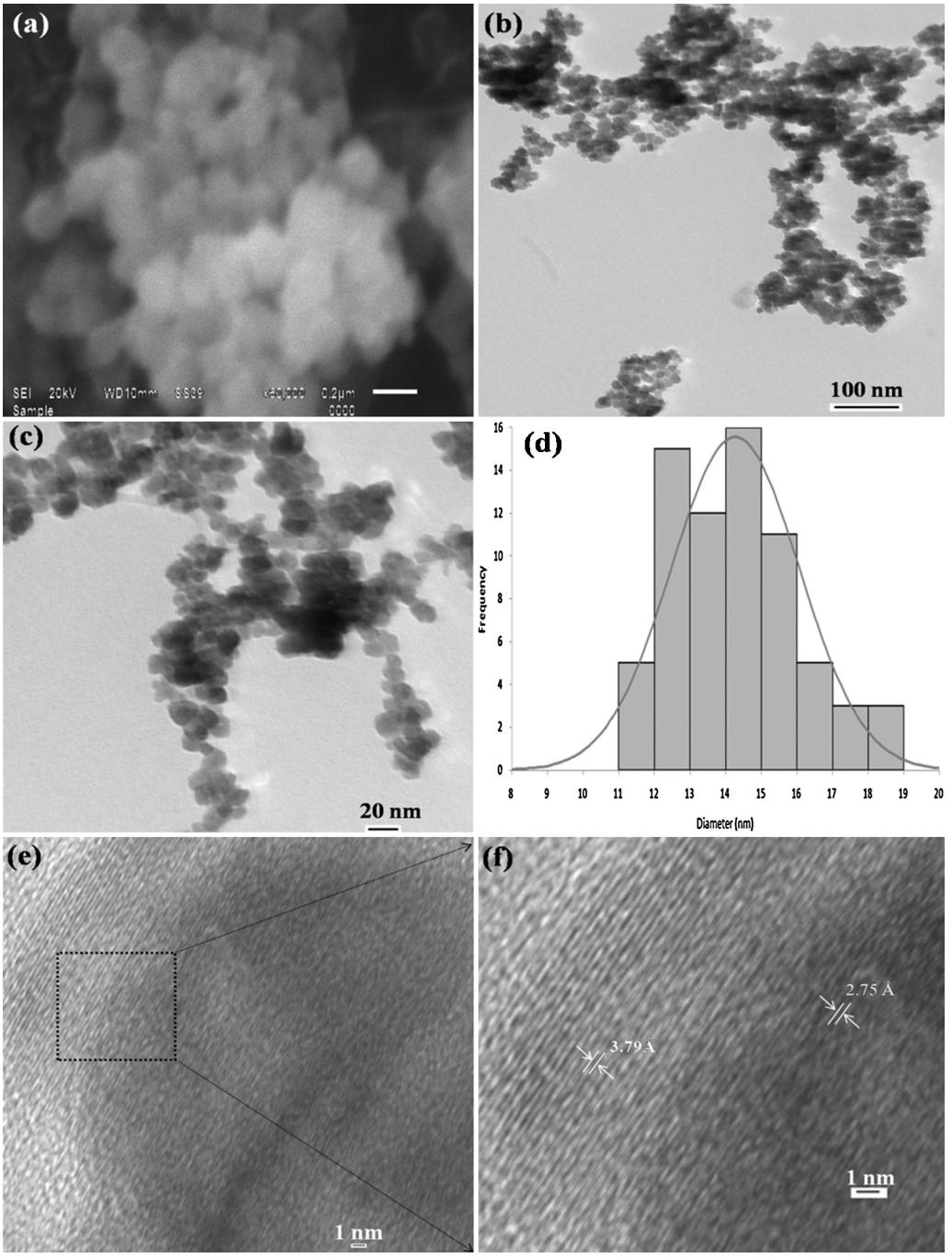

Fig. 5 – (a) SEM, (b and c) TEM micrographs, (d) histogram and (e) HRTEM image, (f) enlarged view of the dotted box of PEG coated potassium ferrite nanoparticles.

thereby resulting in reduced surface energy. As observed in the histogram, Fig. 5 (d), the size distribution ranges from 11 to 19 nm with maximum frequency (diameter of the nanocomposite) in the range 14–15 nm. In Fig. 5(f), the lattice fringes pertaining to PEG and potassium ferrite nanoparticles have been well-observed, thereby confirming the presence of PEG coating on the surface of potassium ferrite nanoparticles.

Magnetic analysis

M–H curve of PEG coated potassium ferrite nanoparticles, as characterized by VSM, Fig. 6, exhibits its superparamagnetic behavior. The magnetic saturation (M_S), remanent magnetization (M_R), and squareness value (M_R/M_S ratio) for uncoated potassium ferrite nanoparticles (as reported in the earlier work (Khanna and Verma, 2013a,b)) as well as for PEG coated potassium ferrite nanoparticles, as obtained, are, respectively, 49.01 emu/g, 4.34 emu/g, 0.08 and 5.78 emu/g, 0.74 emu/g, 0.12. The so-obtained magnetization for potassium ferrite nanoparticles is higher than those reported in the literature (Khanna and Verma, 2014; Sulaiman and Verma, 2012). Superparamagnetic behavior is reflected in less squareness value (Zheng et al., 2005). In non-interacting superparamagnetic particles, the value is 0.5 (Le and Lee, 2011), and for interacting superparamagnetic particles, the dipolar interactions reduce both the magnetic squareness (M_R/M_S ratio) and coercivity (H_C) values due to demagnetizing effect (Franco et al., 2005). Magnetic squareness value related to superparamagnetic behavior is 0.1, i.e., it loses greater than 90% of its magnetism on removal of the applied magnetic field (Schulz et al., 2009). The squareness value obtained for the synthesized PEG coated potassium ferrite nanoparticles is 0.12. Therefore, it exhibits the characteristic feature of superparamagnetism. Less magnetic saturation value is attributed to the chemical combination of non-magnetic layer of PEG on the surface of potassium ferrite nanoparticles. The particle size and its distribution decide the form of magnetization curve, which is further related to the magnetic particle content. A non-magnetic surface coating on the particle reduces the magnetic size as compared to its physical size (Popplewell and Sakhnini, 1995), thus, diminishing the magnetic saturation value. PEG coating on potassium ferrite nanoparticles reduced the magnetic size, and, therefore the magnetic saturation value dropped. Larger size of the nanocomposite results in higher magneto-crystalline anisotropy for the nanocomposite. The magneto-crystalline anisotropy originates from the coupling between electron spins and the angular momentum of the electron orbital (L–S coupling). Superparamagnetic behavior of a particle, which is directly related to its magneto-crystalline anisotropy, is correlated to its L–S coupling, as well (Gubbala et al., 2004; Misra et al., 2004). This is directly proportional to the volume of particles ($EA = KV \sin^2\theta$), where K is the magneto-crystalline anisotropy constant (related to the strength of the L–S coupling), V is the volume of the nanoparticles, and θ is the angle between the magnetization direction and the easy axis of the nanoparticle. EA serves as an energy barrier for blocking the flips of magnetic moments (Gubbala et al., 2004; Misra et al., 2004). The total effective magnetic moment of PEG coated nanoparticles is found to decrease, which is most probably due to a non-collinear spin structure originating from the pinning of the surface spins and PEG coating at the interface of nanoparticles (Kim et al., 2001). However, coating of the nanoparticles with PEG did not affect the superparamagnetic nature of the synthesized potassium ferrite nanoparticles, as observed in Fig. 5.

Lim et al. (2008), synthesized various types of water soluble PEGylated magnetic complexes (PMCs) and the saturation magnetization at 1.0 T were 2.1 emu/g (mPEG-lauric acid (PLMs)), 2.1 emu/g (mPEG-stearic acid (PSMs)) and 2.0 emu/g (mPEG-oleic acid (POMs)), respectively. Mukhopadhyay et al. (2012), synthesized PEG coated magnetite (Fe_3O_4) nanoparticles (PEG4K-NP and PEG20K-NP) for prevention of the reduction of cytochrome C, these exhibited room temperature

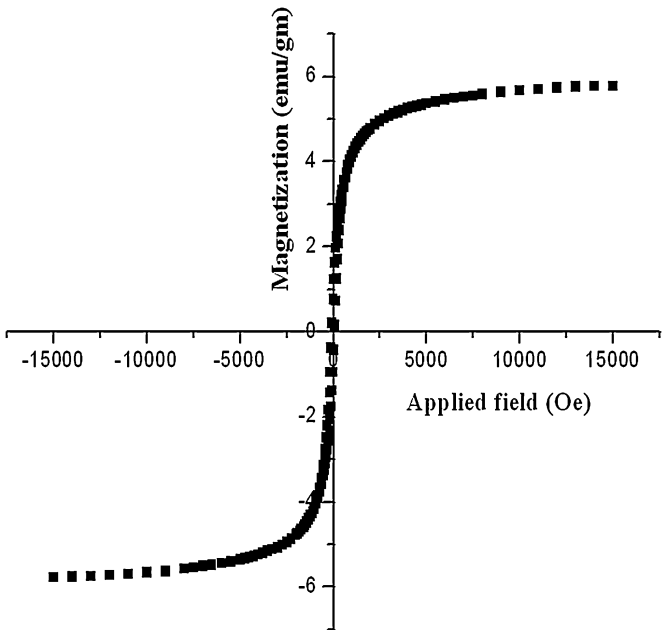

Fig. 6 – M–H curve of PEG coated potassium ferrite nanoparticles.

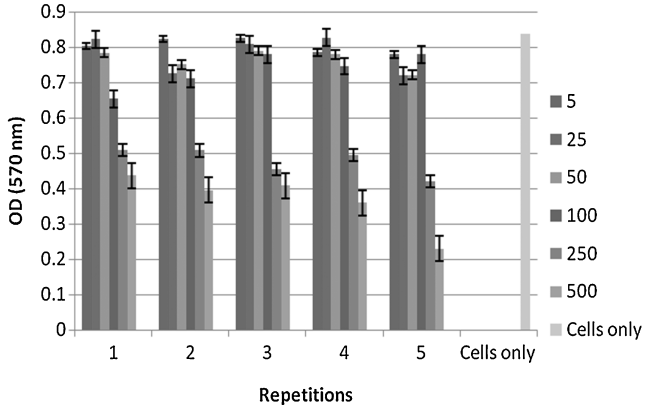

Fig. 7 – Optical density (OD) at 570 nm of all repetitions at all concentrations. (For colour resolution see the online edition.)

(300 K) ferromagnetism with magnetic saturation value of 50 and 43 emu/g. Also, Karaoglu et al. (2011), synthesized PEG-Mn_3O_4 nanoparticles which exhibited paramagnetic-like behavior and did not saturate even at the maximal field. Superparamagnetic behavior of PEG-magnetic complexes has not been reported so far. This was the motivation for the present study, wherein PEG-$KFeO_2$ nanocomposite exhibited superparamagnetic behavior with magnetic saturation value of 5.78 emu/g, which is required for biomedical applications.

In vitro cytotoxicity analysis

Dose-dependent cytotoxicity of the nanocomposite tested on T-cell lines (Jurkat cells) using MTT assay reveals their non-toxic behavior. Fig. 7 shows the optical density (OD) values of all repetitions at all concentrations. The cell viabilities at 5, 25, 50, 100, 250, 500 μg/ml, as calculated by Eq. (1), are, respectively, 95.9%, 93.1%, 91.3%, 87.6%, 57%, 43.6%. Each data point in Fig. 8 was obtained by averaging the values obtained from five wells. In Fig. 8, the statistical analysis using paired *t*-test [1] has been determined to scrutinize the effect of synthesized nanocomposite on the cells. PEG is a well known biocompatible material and it leads to reduced agglomeration. Therefore, the enhanced cell viability is attributed to these two factors, which encourages their intracellular uptake and reduced cellular damage (Singh et al., 2012). A significant cell viability has been observed below 250 μg/ml, and, a fall occurs at 250 μg/ml; this may be attributed to scarcity of culture media during the growth of the cells while running the assay, rather than any toxicity of the synthesized nanocomposite. On interaction, the nanocomposite first attaches to cells, then is internalized by endocytosis, finally gets accummulated in digestive vacuoles (Tomitaka et al., 2009). Therefore, at higher concentration, the overloading of particles possibly caused cell death.

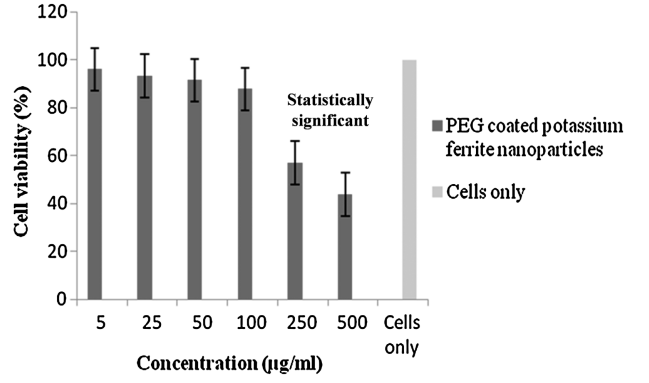

Fig. 8 – Mean cell viability (%) as determined by MTT assay.

Conclusions

This paper reports the coating of polymer PEG on potassium ferrite nanoparticles. The XRD pattern reveals the formation of orthorhombic structure of $KFeO_2$ with additional peaks at 19° and 23°, characteristic of PEG. The characteristic bands of PEG, in the IR spectrum, confirm its coating on the nanoparticles' surface. The decomposition of PEG polymer shifts to higher temperature due to the formation of covalent bonds with potassium ferrite nanoparticles. SEM and TEM micrographs reveal the spherical morphology and reduced agglomeration of the synthesized nanocomposite. The lattice fringes corresponding to PEG and potassium ferrite nanoparticles in the HRTEM micrograph reiterate the confirmation of coating. Superparamagnetism with magnetic saturation of 5.78 emu/g is observed in the M–H curve of the synthesized nanocomposite. Dose-dependent cellular toxicity reveals that the nanocomposite exhibits non-toxicity below 250 μg/ml but at higher concentrations, the cell viability decreased probably due to overloading of the nanoparticles. Owing to the size distribution, superparamagnetism and biocompatibility, the synthesized nanocomposite finds potential applications in drug delivery and hyperthermia but not in Magnetic resonance imaging where size in the range of 5–10 nm is required.

Conflict of interest

None declared.

Acknowledgement

One of the authors, Lavanya Khanna, gratefully acknowledges Department of Science and Technology, Government of India, New Delhi for awarding her INSPIRE Fellowship to carry out this research work.

REFERENCES

Ahmed, M.A., Okasha, N., Mansour, S.F., El-dek, S.I., 2010. Bi-modal improvement of the physico-chemical characteristics of PEG and MFe_2O_4 subnanoferrite. J. Alloys Compd. 496, 345–350.

Arruebo, M., Pacheco, R.F., Ibarra, M.R., Santamaria, J., 2007. Magnetic nanoparticles for drug delivery. Nanotoday 2, 22–32.

Baldi, G., Bonacchi, D., Franchini, M.C., Gentili, D., Lorenzi, G., Ricci, A., Ravagli, C., 2007. Synthesis and coating of cobalt ferrite nanoparticles: a first step toward the obtainment of new magnetic nanocarriers. Langmuir 23, 4026–4028.

Čampelj, S., Makovec, D., Drofenik, M., 2009. Functionalization of magnetic nanoparticles with 3-aminopropyl silane. J. Magn. Magn. Mater. 321, 1346–1350.

Ciabatti, I., Tognotti, F.L., Lombardi, L., 2010. Treatment and reuse of dyeing effluents by potassium ferrate. Desalination 250, 222–228.

Durmus, Z., Tomaş, M., Baykal, A., Kavas, H., Toprak, M.S., 2011. PEG-assisted synthesis of Mn_3O_4 nanoparticles: a structural and magnetic study. Synth. React. Inorg. Metal-Org. Nano-Metal Chem. 41, 768–773.

Echevarria, I.M.R., Selvestrel, F., Segat, D., Guarino, G., Tavano, R., Causin, V., Reddi, E., Papini, E., Mancin, F., 2010. Highly PEGylated silica nanoparticles: ''ready to use'' stealth functional nanocarriers. J. Mater. Chem. 20, 2780–2787.

Feng, B., Hong, R.Y., Wang, L.S., Guo, L., Li, H.Z., Ding, J., Zheng, Y., Wei, D.G., 2008. Synthesis of Fe_3O_4/APTES/PEG diacid functionalized magnetic nanoparticles for MR imaging. Colloids Surf. A: Physicochem. Eng. Asp. 328 (2008), 52–59.

Franco, V., Conde, C.F., Conde, A., Kiss, L.F., 2005. Relationship between coercivity and magnetic moment of superparamagnetic particles with dipolar interaction. Phys. Rev. B 72 (174424), 1–10.

Gozuak, F., Koseoglu, Y., Baykal, A., Kavas, H., 2009. Synthesis and characterization of $Co_xZn_{1-x}Fe_2O_4$ magnetic nanoparticles via a PEG-assisted route. J. Magn. Magn. Mater. 321, 2170–2177.

Gubbala, S., Nathani, H., Koizol, K., Misra, R.D.K., 2004. Magnetic properties of nanocrystalline Ni–Zn, Zn–Mn, and Ni–Mn ferrites synthesized by reverse micelle technique. Physica B 348, 317–328.

Gupta, A.K., Gupta, M., 2005. Synthesis and surface engineering of iron oxide nanoparticles for biomedical applications. Biomaterials 26, 3995–4021.

Jiang, J.Q., Panagoulopoulos, A., Bauer, M., Pearce, P., 2006. The role of potassium ferrate(VI) in the inactivation of *Escherichia coli* and in the reduction of COD for water remediation. J. Environ. Manage. 79, 215–220.

Karaoglu, E., Deligoz, H., Sozeri, H., Baykal, A., Toprak, M.S., 2011. Hydrothermal synthesis and characterization of PEG-Mn_3O_4 nanocomposite. Nano-Micro Lett. 3, 25–33.

Khanna, L., Verma, N.K., 2013a. PEG/$CaFe_2O_4$ nanocomposite: structural, morphological, magnetic and thermal analyses. Physica B 427, 68–75.

Khanna, L., Verma, N.K., 2013b. Silica/potassium ferrite nanocomposite: structural, morphological, magnetic, thermal and *in vitro* cytotoxicity analysis. Mater. Sci. Eng. B 178, 1230–1239.

Khanna, L., Verma, N.K., 2014. Synthesis, characterization and biocompatibility of potassium ferrite nanoparticles. J. Mater. Sci. Technol. 30, 30–36.

Kim, D.K., Zhang, Y., Voit, W., Rao, K.V., Muhammed, M., 2001. Synthesis and characterization of surfactant-coated superparamagnetic monodispersed iron oxide nanoparticles. J. Magn. Magn. Mater. 225, 30–36.

Koo, O.M., Rubinstein, I., Onyuksel, H., 2005. Role of nanotechnology in targeted drug delivery and imaging: a concise review. Nanomed.: Nanotechnol. Biol. Med. 1, 193–212.

Larumbe, S., Landazabal, J.I.P., Pastor, J.M., Polo, C.G., 2012. Sol–gel $NiFe_2O_4$ nanoparticles: effect of the silica coating. J. Appl. Phys. 111, 103911.

Le, K.W., Lee, C.E., 2011. Triggering a metal-insulator transition in $La_{0:8}Sr_{0:2}MnO_3$ nanoparticle-decorated carbon nanotubes. J. Korean Phys. Soc. 59, L1–L5.

Lee, J., Choa, Y.H., Kim, J., Kim, K.H., 2011. Comparison of the magnetic properties for the surface-modified magnetite nanoparticles. IEEE Trans. Magn. 47, 2874–2877.

Leung, K.C.F., Wang, Y.X.J., 2010. Mn–Fe nanowires towards cell labeling and magnetic resonance imaging. In: Lupu, N. (Ed.), Nanowires Science and Technology. InTecH, Croatia, pp. 331–344.

Lim, E.K., Yang, J., Park, M.Y., Park, J., Suh, J.S., Yoon, H.G., Huh, Y.M., Haam, S., 2008. Synthesis of water soluble PEGylated magnetic complexes using mPEG-fatty acid for biomedical applications. Colloids Surf. B 64, 111–117.

Lim, M., Kim, M.J., 2010. Effectiveness of potassium ferrate (K_2FeO_4) for simultaneous removal of heavy metals and natural organic matters from river water. Water Air Soil Pollut. 211, 313–322.

Ling, F., Wang, J.G., Liu, Q.F., Li, M., Ye, L.T., Gong, X.N., 2010. Prevention of Ichthyophthirius multifiliis infestation in goldfish (*Carassius auratus*) by potassium ferrate(VI) treatment. Vet. Parasitol. 168, 212–216.

Lipka, J., Behnke, M.S., Sperling, R.A., Wenk, A., Takenaka, S., Schleh, C., Kissel, T., Parak, W.J., Kreyling, W.G., 2010. Biodistribution of PEG-modified gold nanoparticles following intratracheal instillation and intravenous injection. Biomaterials 31, 6574–6581.

Ma, F., Lu, J., Wang, Z., Sun, J., Gong, Q., Song, B., Ai, H., Gu, Z., 2010. Encapsulation of $MnFe_2O_4$ nanoparticles with amphiphilic PEG-lipid micelles as novel MRI probes. Int. J. Magn. Reson. Imaging 2, 50–55.

McBain, S.C., Yiu, H.H.P., Dobson, J., 2008. Magnetic nanoparticles for gene and drug delivery. Int. J. Nanomed. 3, 169–180.

Misra, R.D.K., Gubbala, S., Kale, A., Egelhoff Jr., W.F., 2004. A comparison of the magnetic characteristics of nanocrystalline nickel, zinc, and manganese ferrites synthesized by reverse micelle technique. Mater. Sci. Eng. B 111, 164–174.

Mohapatra, S., Rout, S.R., Maiti, S., Maiti, T.K., Panda, A.B., 2011. Monodisperse mesoporous cobalt ferrite nanoparticles: synthesis and application in targeted delivery of antitumor drugs. J. Mater. Chem. 21, 9185–9193.

Mukhopadhyay, A., Joshi, N., Chattopadhyay, K., De, G., 2012. A facile synthesis of PEG-coated magnetite (Fe_3O_4) nanoparticles and their prevention of the reduction of cytochrome C. Appl. Mater. Interfaces 4, 42–149.

Phadatare, M.R., Khot, V.M., Salunkhe, A.B., Thorat, N.D., Pawar, S.H., 2012. Studies on polyethylene glycol coating on $NiFe_2O_4$ nanoparticles for biomedical applications. J. Magn. Magn. Mater. 324, 770–772.

Popplewell, J., Sakhnini, L., 1995. The dependence of the physical and magnetic properties of magnetic fluids on particle size. J. Magn. Magn. Mater. 149, 72–78.

Rana, S., Gallo, A., Srivastava, R.S., Misra, R.D.K., 2007. On the suitability of nanocrystalline ferrites as a magnetic carrier for drug delivery: functionalization, conjugation and drug release kinetics. Acta Biomater. 3, 233–242.

Rana, S., Philip, J., Raj, B., 2010. Micelle based synthesis of cobalt ferrite nanoparticles and its characterization using Fourier transform infrared transmission spectrometry and thermogravimetry. Mater. Chem. Phys. 124, 264–269.

Rastogi, R., Gulati, N., Kotnala, R.K., Sharma, U., Jayasundar, R., Koul, V., 2011. Evaluation of folate conjugated PEGylated thermosensitive magnetic nanocomposites for tumor imaging and therapy. Colloids Surf. B 82, 160–167.

Schulz, D.L., Sailer, R.A., Caruso, A.N., 2009. Superparamagnetic transition metal iron oxygen nanoparticles. U. S. Patent No. 20090194733.

Silverstein, R., Webster, M., Kiemle, F.X.D.J., 2005. Spectrometric Identification of Organic Compounds, 7th ed. John Wiley & Sons, Inc, United States of America.

Singh, N., Karambelkar, A., Gu, L., Lin, K., Miller, J.S., Chen, C.S., Sailor, M.J., Bhatia, S.N., 2011. Bioresponsive Mesoporous Silica Nanoparticles for Triggered Drug Release. J. Am. Chem. Soc. 133, 19582–19585.

Singh, R.K., Kim, T.H., Patel, K.D., Knowles, J.C., Kim, H.W., 2012. Biocompatible magnetite nanoparticles with varying silica-coating layer for use in biomedicine: physicochemical and magnetic properties, and cellular compatibility. J. Biomed. Mater. Res. A 100, 1734–1742.

Sulaiman, N.H., Verma, N.K., 2012. Synthesis of Silica Coated Potassium Ferrite Nanoparticles for Biomedical Applications. (Master thesis)Thapar University.

Sun, C., Du, K., Fang, C., Bhattarai, N., Veiseh, O., Kievit, F., Stephen, Z., Lee, D., Ellenbogen, R.G., Ratner, B., Zhang, M., 2010. PEG-mediated synthesis of highly dispersive multifunctional superparamagnetic nanoparticles: their physicochemical properties and function *in vivo*. ACS Nano 4 (4), 2402–2410.

Sun, Y., Duan, L., Guo, Z., DuanMu, Y., Ma, M., Xu, L., Zhang, Y., Gu, N., 2005. An improved way to prepare superparamagnetic magnetite-silica core–shell nanoparticles for possible biological application. J. Magn. Magn. Mater. 285, 65–70.

Tejamaya, M., Römer, I., Merrifield, R.C., Lead, J.R., 2012. Stability of Citrate, PVP, and PEG coated silver nanoparticles in ecotoxicology media. Environ. Sci. Technol. 46, 7011–7017.

Tomitaka, A., Hirukawa, A., Yamada, T., Morishita, S., Takemura, Y., 2009. Biocompatibility of various ferrite nanoparticles evaluated by *in vitro* cytotoxicity assays using HeLa cells. J. Magn. Magn. Mater. 321, 1482–1484.

Veiseh, O., Gunn, J.W., Zhang, M., 2010. Design and fabrication of magnetic nanoparticles for targeted drug delivery and imaging. Adv. Drug Deliv. Rev. 62, 284–304.

Yallapu, M.M., Othman, S.F., Curtis, E.T., Gupta, B.K., Jaggi, M., Chauhan, S.C., 2011. Multi-functional magnetic nanoparticles for magnetic resonance imaging and cancer therapy. Biomaterials 32, 1890–1905.

Yang, H., Zhang, C., Shi, X., Hu, H., Du, X., Fang, Y., Ma, Y., Wu, H., Yang, S., 2010. Water-soluble superparamagnetic manganese ferrite nanoparticles for magnetic resonance imaging. Biomaterials 31, 3667–3673.

Yin, H., Too, H.P., Chow, G.M., 2005. The effects of particle size and surface coating on the cytotoxicity of nickel ferrite. Biomaterials 26, 5818–5826.

Zampori, L., Dotelli, G., Stampino, P.G., Cristiani, C., Zorzi, F., Finocchio, E., 2012. Thermal characterization of a montmorillonite, modified with polyethylene-glycols (PEG1500 and PEG4000), by in situ HT-XRD and FT IR: formation of a high-temperature phase. Appl. Clay Sci. 59–60, 140–147.

Zhang, J., Rana, S., Srivastava, R.S., Misra, R.D.K., 2008. On the chemical synthesis and drug delivery response of folate receptor-activated, polyethylene glycol-functionalized magnetite nanoparticles. Acta Biomater. 4, 40–48.

Zhang, X.D., Wu, D., Shen, X., Liu, P.X., Yang, N., Zhao, B., Zhang, H., Sun, Y.M., Zhang, L.A., Fan, F.Y., 2011. Size-dependent *in vivo* toxicity of PEG-coated gold nanoparticles. Int. J. Nanomed. 6, 2071–2081.

Zheng, W., Gao, F., Gu, H., 2005. Magnetic polymer nanospheres with high and uniform magnetite content. J. Magn. Magn. Mater. 288, 403–410.

WEB REFERENCE

https://statistics.laerd.com/calculators/dependent-t-test-paired-samples-calculator.php (accessed 19.10.13).